



OPEN

Diversity analysis of sea anemone peptide toxins in different tissues of *Heteractis crispa* based on transcriptomics

Qiqi Guo¹, Jinxing Fu¹, Lin Yuan^{1,3}, Yanling Liao¹, Ming Li¹, Xinzhong Li², Bo Yi³, Junqing Zhang¹✉ & Bingmiao Gao¹✉

Peptide toxins found in sea anemones venom have diverse properties that make them important research subjects in the fields of pharmacology, neuroscience and biotechnology. This study used high-throughput sequencing technology to systematically analyze the venom components of the tentacles, column, and mesenterial filaments of sea anemone *Heteractis crispa*, revealing the diversity and complexity of sea anemone toxins in different tissues. A total of 1049 transcripts were identified and categorized into 60 families, of which 91.0% were proteins and 9.0% were peptides. Of those 1049 transcripts, 416, 291, and 307 putative proteins and peptide precursors were identified from tentacles, column, and mesenterial filaments respectively, while 428 were identified when the datasets were combined. Of these putative toxin sequences, 42 were detected in all three tissues, including 33 proteins and 9 peptides, with the majority of peptides being ShKT domain, β -defensin, and Kunitz-type. In addition, this study applied bioinformatics approaches to predict the family classification, 3D structures, and functional annotation of these representative peptides, as well as the evolutionary relationships between peptides, laying the foundation for the next step of peptide pharmacological activity research.

Sea anemones (Cnidaria: Anthozoa: Hexacorallia: Actiniaria) are an order of marine animals found in deep oceans and shallow coastal regions around the world, including two suborders: Anenthemonae and Enthemonae¹. Cnidarians are one of the oldest venomous lineages in existence. Molecular and fossil evidence suggesting that they appeared more than 750 million years ago, before the Ediacaran period^{2–4}. Like other cnidarians, sea anemones store venom in specialized cells known as nematocysts, which have venom-filled capsules and inverted tubules^{5,6}. Contact with prey causes an explosive eversion of the tubule, piercing the target organism and releasing venom for predation, defense, or competitive deterrence⁷. The endodermal and ectodermal gland tissue of sea anemones contains venom, revealing an alternative venom-delivery mechanism in sea anemones^{8,9}.

Sea anemone venom contains complex proteinaceous (peptides and proteins) and non-proteinaceous components (e.g., quaternary ammonium compounds, purines, and biogenic amines)¹⁰. Sea anemone toxins disrupt many targets, including voltage-gated sodium (Nav) and potassium (Kv) channels, acid-sensing ion channels (ASIC), transient receptor potential vanilloid 1 (TRPV1), and transient receptor potential ankyrin 1 (TRPA1)^{11–15}. Many peptide toxins in sea anemones have been studied for their potential as pharmaceutical tools or treatments. The sea anemone venom protein ShK of *Stichodactyla helianthus* inhibited Kv1.3 with an IC₅₀ in the low picomolar range^{16,17}. The efficacy of ShK and its homologs in the treatment of human autoimmune disorders, including rheumatoid arthritis, multiple sclerosis, and type I diabetes, have been demonstrated in animal models^{18–20}. Moreover, the phase I trials of Dalazatide (formerly ShK-186) in the treatment of psoriasis have been successfully concluded²¹.

Sea anemone *Heteractis crispa* (*H. crispa*), also known as the leathery sea anemone, long tentacle anemone or purple tip anemone, belongs to Heteractidae family and is native to the Indo-Pacific region^{22–24}. In 1994, Mebs mentioned the sea anemone *Heteractis crispa*²⁵, which has the valid name *Radianthus crispa* on the WoRMS

¹Engineering Research Center of Tropical Medicine Innovation and Transformation, Ministry of Education, International Joint Research Center of Human-machine Intelligent Collaborative for Tumor Precision Diagnosis and Treatment of Hainan Province, School of Pharmacy, Hainan Medical University, Haikou, China. ²School of Health and Life Sciences, Teesside University, Middlesbrough, UK. ³Department of Pharmacy, 928th Hospital of PLA Joint Logistics Support Force, Haikou, China. ✉email: hy0207002@hainmc.edu.cn; gaobingmiao@hainmc.edu.cn

website. In 2010, Fedorov *et al.* published an article in which they mentioned that *Radianthus macrodactylus* is equivalent to *Heteractis crispa*²⁶. Some toxins have been detected in *H. crispa*, mainly actinoporin, Kunitz-type protease inhibitors, Nav channel toxins, and Kv channel toxins^{26–29}, and the venom assembly in the tentacles, mesentery filaments, and columns of three species of sea anemones (*Anemonia sulcata*, *H. crispa*, and *Megalactis griffithsi*) has been investigated, and the number of toxin-like genes varies significantly between tissues and species^{22,30,31}. The high-throughput sequencing (HTS) technology has been increasingly applied in studying sea anemone venom components, such as *Stichodactyla haddoni* and *Anthopleura dowii*^{32–34}. In this study, we applied HTS technology to identify the protein and peptide components in *H. crispa* and compared the distribution of peptide toxins in different tissues, this lays the foundation for in-depth research on *H. crispa* peptide toxins and provides new potentials for marine drug development.

Results

Transcriptome sequence assembly

We applied the BUSCO suite tools to assess the completeness of transcriptomes³⁵. We found that overall, the BUSCO match values were within the expected range for both a complete single copy and duplicated copies of BUSCO (S/D). Whether in the Tentacles, Column, Mesenterial filaments, or their combination (Combine) dataset, there were a large number of Complete BUSCOs (C) accounting for more than 90% of the Total BUSCO groups, while the proportion of Fragmented BUSCOs (F) and Missing BUSCOs (M) in the Total BUSCO groups was extremely low (Table S1).

The sequence and assembly of *H. crispa* transcriptome were generated and then submitted to the National Center for Biotechnology Information (NCBI) (BioProject: PRJNA893400, and SRA accession: SRX17999840, SRX17999841, and SRX17999842). The total Reads of the Tentacles (83,799,076), Column (69,427,990), and Mesenterial filaments (67,486,092) were merged into one combined dataset (Combine). After filtering out low-quality reads, about 81.9 million (81,961,116), 67.8 million (67,828,874), 66.2 million (66,235,446), and 120 million reads were obtained from the Tentacles, Column, Mesenterial filaments, and the Combine dataset, respectively. The HTS data was assembled into transcript sequences by using Inchworm, Chrysalis, and Butterfly assembly tools^{36,37} which generated 288,563 contigs with a mean length of 1,001 bp and an N50 length of 1,829 bp. Meanwhile, 183,198 non-redundant unigenes with a mean length of 769 bp and an N50 length of 1,199 bp were obtained by splicing and removing redundant sequences (Table S2).

Annotation was performed based on five databases to examine unigene functions: Nr (NCBI non-redundant protein sequence), KOG (Eukaryotic Orthologous Groups), Uniprot (Universal Protein), GO (Gene Ontology), and KEGG (Kyoto Encyclopedia of Genes and Genomes). A total of 183,198 unigenes were grouped into these databases: Nr (37,932 unigenes), Uniprot (40,920 unigenes), GO (29,531 unigenes), KEGG (16,167 unigenes), and KOG (20,259 unigenes) respectively, while there were 139,585 unigenes lacking annotation in these databases (Figure S1). Moreover, 19,414 unigenes were enriched into 33 KEGG pathways and assigned into five primary categories: processing environmental information (2,799, 14.42%), cellular processes (2,801, 14.42%), genetic information processing (2,539, 13.08%), metabolism (6,221, 32.04%), and organismal systems (5,054, 26.03%). Most of these unigenes were assigned to metabolism, and the global and overview maps of metabolism contained the most annotated unigenes (Figure S2). 18,016 unigenes were annotated in KOG and categorized into 25 different molecular families (Figure S3). "General function cluster prediction only" (3,831 unigenes, 21.26%) was the largest of these KOG categories, followed by "Signal transduction pathways" (2,419 unigenes, 13.43%), "Posttranslational modification, protein turnover, chaperones" (1,893 unigenes, 10.51%), and "Nuclear structure" (10 unigenes, 0.06%). GO analysis demonstrated that 110,279 unigenes were categorized into three categories: Cellular Component (27,969, 25.36%), Biological Process (46,361, 42.13%), and Molecular Function (35,849, 32.51%), which were further classified into 49 functional groups. The top four enriched functional groups were binding (14,521 unigenes), cellular process (14,127 unigenes), catalytic activity (13,471 unigenes), and metabolic function (13,024 unigenes) (Figure S4).

Hierarchical clustering analysis demonstrated that the Tentacles, Column, and Mesenterial filaments in *H. crispa* were well distinguished, and all gene sequences were divided into three categories (Fig. 1a). GO analysis of gene expression indicated (Fig. 1b–d) that the number of genes expressed in Tentacles was greater than the number of genes expressed in the Column and Mesenterial filaments. In Tentacles, ribosomes, structural constitutions of ribosomes, translation, and internal anatomical structure have the largest number of genes. Meanwhile, the extracellular region and proteolysis have the largest gene numbers in the Column and Mesenterial filaments.

Family classification of proteins and peptide toxins in the *H. crispa* transcriptome

A total of 1049 transcripts were assessed and categorized into 60 families regarding predicted functions, which were assessed according to their amino acid sequence identity, of which 91.0% were proteins and 9.0% were peptides (amino acids \leq 80) (Fig. 2, Table S3). Most protein components matched Peptidase S1, metalloprotease, G-protein coupled receptor, and Factor 5/8 C-domain. The important and well-known actinoporins family was included in the above statement (Figures S5,6). Moreover, the peptide components were related to the ShKT domain, β -defensin, and Kunitz-type.

Comparative analysis of protein and peptide toxins in different tissues of *H. crispa*

A total of 416, 291, 307, and 428 putative proteins and peptide toxins precursors were detected from the tentacles, column, mesenterial filaments, and their combined dataset, respectively. Figure 3a depicts the comparative distributions of protein and peptide toxins. Of these putative proteins and toxic precursors, 42 were common in these four datasets, of which 33 were proteins and 9 were peptides. A total of 81 were shared by tentacles and column, 74 were shared by tentacles and mesenterial filaments, and 74 were common in both column and mesenterial

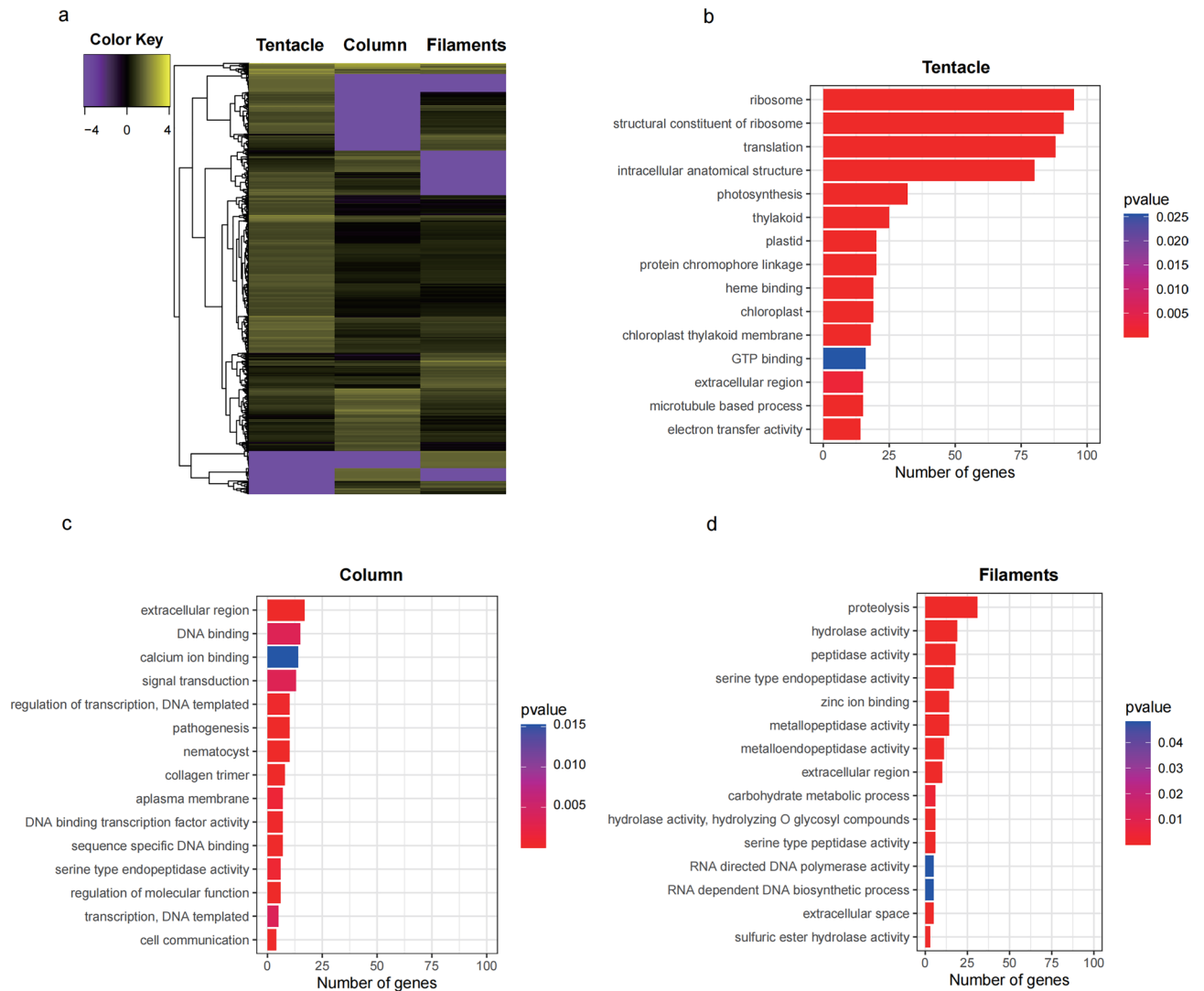


Figure 1. Cluster heatmap and genes annotated by GO analysis in three different tissues. **(a)** Cluster heatmap of three different tissues. **(b)** Bar chart of the number of genes in tentacles. **(c)** Bar chart of the number of genes in the column. **(d)** Bar chart of the number of genes in the mesenterial filaments.

filaments. These 42 common toxins precursors across four databases were classified into 14 families: β -defensin, metalloproteinase, Kunitz-type, and ShKT domain (Fig. 3b). For each protein and peptide toxin, transcripts Per Kilobase of exon model per Million mapped reads (TPM) values were calculated representing transcription levels. The top ten protein and peptide toxins (with the highest TPM values) in each dataset were assigned. The metalloproteinase and ShKT domains derived from the tentacles were expressed at high levels, while the ShKT domain, metalloproteinase, and β -defensin derived from the column were expressed at high levels too. However, various proteins and peptide toxins derived from mesenterial filaments were downregulated, among which metalloproteinase and ShKT domains were still the highest (Fig. 3c). Therefore, protein and peptide toxins in the ShKT domain and metalloproteinase were highly expressed in three *H. crispa* tissues. Additionally, the ShKT domain included protein and peptide toxins with the highest expressions in the column. Surprisingly, only β -defensin-like peptides were highly expressed in the column but not in the other two tissues, which deserves further studies.

Cysteine pattern analysis of sea anemone peptide toxins

The nomenclature and classification of cysteine patterns in sea anemone neurotoxic peptides have been reported by Kozlov³⁸ and Gao et al.³⁹. In this study, a total of 93 peptide toxins were obtained from the tentacles, column, mesenterial filaments, and combined datasets and named Hc-01~Hc-93 in order (Table S4). Many cysteines exist in sea anemone peptide toxins, and cysteine structural scaffolds are diverse. According to our previously proposed classification method^{39,40}, cysteine patterns of these 93 peptides were split into eight broad categories and several subcategories (Fig. 4). The most common peptide structures have six cysteines and three disulfide bond patterns (VI), accounting for 47.31% followed by those having four cysteines producing two disulfide bond patterns (IV), accounting for 25.81%. Furthermore, although most peptides possess an even number of cysteines, there is a small proportion of peptides characterized by an odd number of cysteine residues. The peptide toxins of

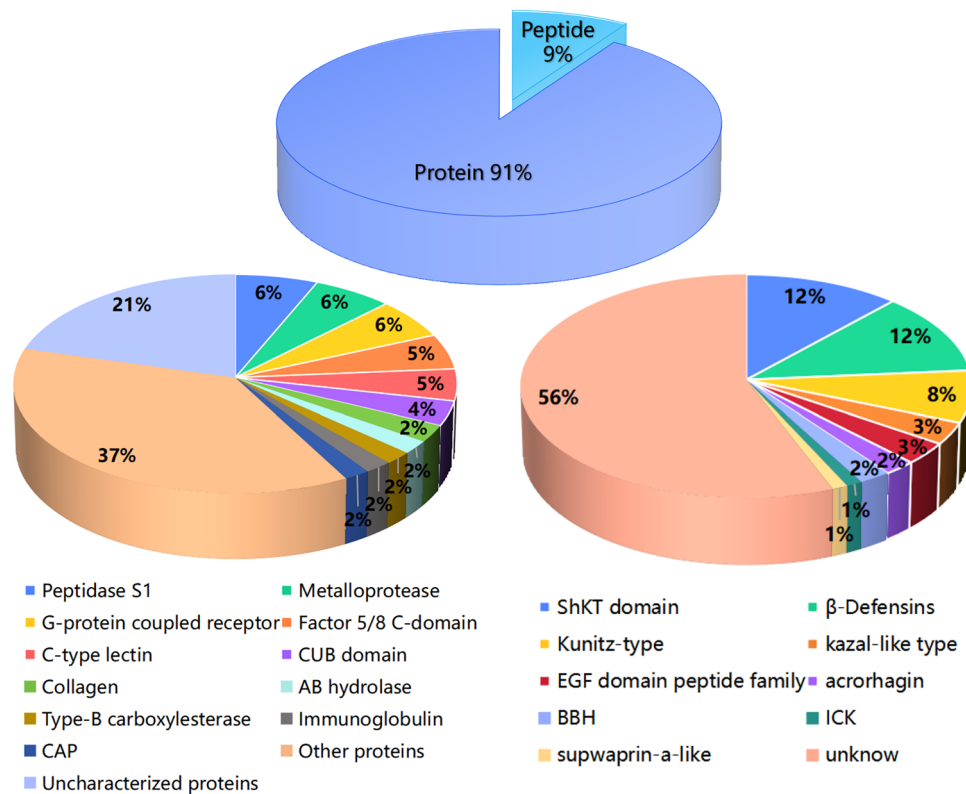


Figure 2. Families of putative protein and peptide toxins in *H. crispa* transcriptome. Based on their amino acid sequences and cysteine scaffolds, the 956 protein sequences and 93 peptide sequences with significant BLAST hits to manually curated lists of animal toxins in UniProt (www.uniprot.org/program/Toxins) were assigned to distinct toxin families.

IV-type and VI-type in sea anemones may be engaged in capturing prey, defending against predators, or repulsing competitors, indicating that these peptide toxins have rich targeting activities^{41,42}. These peptide toxins have potential biotechnological applications and provide rich resources for the development of new drugs.

Sequence analysis of typical sea anemone peptide toxins

Sea anemone venom has a high concentration of peptide toxins, serving a crucial function in prey and defense⁷, and they operate on various ion channels, such as Nav channels, Kv channels, ASIC, TRPV1, and TRPA1^{29,43–45}. The three-dimensional (3D) structure or cysteine pattern or both of nine representative anemone peptide toxins have been determined, including ShKT domain, epidermal growth factor-like (EGF-like), β-defensin-like, Kunitz-type, *Anemonia sulcata* toxin III (ATX-III), inhibitor cystine-knot (ICK), small cysteine-rich peptides (SCRiPs), proline-hinged asymmetric β-hairpin (PHAB), and boundless β-hairpin (BBH)⁴¹. Herein, we described sea anemone peptide toxins with typical and unique homologs, including ShKT domain (11 homologs), β-defensin-like (11 homologs), Kunitz-type (7 homologs), and EGF-like (3 homologs). The peptide toxin sequences from these representative families were analysed to assess their similarity. The distribution of these sequences in these four datasets was examined. Additionally, the 3D structures of select significant peptide toxins were predicted (Figs 5, 6, 7 and 8).

The ShK toxin, isolated from the sea anemone *Stichodactyla helianthus*⁴⁶, is termed the ShKT domain inhibits Kv channels^{16,17,47–50}. A total of 11 homologous sequences with ShK that have not been reported previously were assessed, their cysteine pattern was C-C-C-CX3CX2C, and it predicted that the connection mode of disulfide bonds was C1-C6, C2-C4, C3-C5 (Fig. 5a,b). The sequence alignment demonstrated that HC-39 had the highest similarity with the previously identified sequence ID (GenBank No. XP_031556600.1), and the sequence identity was 85.71%. Additionally, the sequence similarity of HC-36/37/43 with ShK was 30.77%, 52.94%, and 30.30%, respectively. The homology modeling prediction indicated that HC-36/37/43 and ShK have 3D structure similarities. This suggests they may simultaneously act on Kv channels (Fig. 5c). These peptide sequences are all analogues of ShK and deserve further study.

β-defensins are ubiquitous in vertebrate antimicrobial peptides and are part of the main components of the innate immune system^{51–53}. However, β-defensin-like peptides in sea anemone venom including CgNa, Rc I, Am II, BDS I, APETx1, APETx2, and Magnificamide are potential toxins that may disrupt voltage- and ligand-gated ion channels as Nav types 1/2/4, Kv type 3, ASIC, and ASIC3^{54–60}. CgNa can be purified from the sea anemone *Condylactis gigantea* and inhibit Nav types 1/2⁶¹. Rc I is a peptide toxin in *H. crispa*, which can inhibit Nav channels⁶². Am II is a neurotoxin from *Antheopsis maculata* with toxin-paralyzing activity against crabs⁶³.

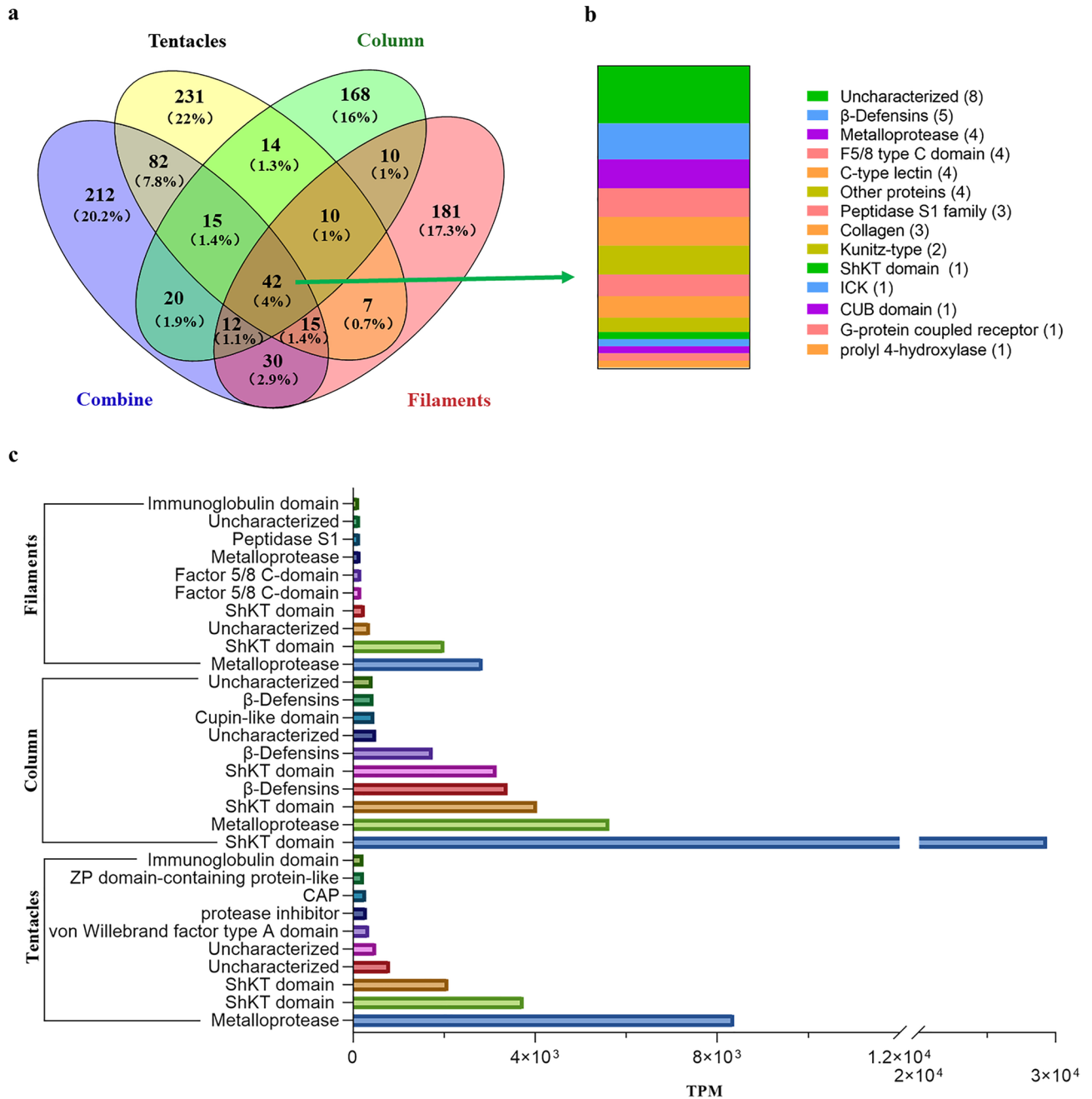


Figure 3. Transcripts of protein and peptide toxins from several *H. crispa* tissues are compared. **(a)** Correlation between datasets of putative protein and neurotoxic peptide detected from *H. crispa* combine, tentacles, column, and mesenterial filaments. **(b)** 42 putative protein and peptide transcripts from various *H. crispa* tissues. **(c)** The ten most greatly expressed protein and peptide transcripts from different *H. crispa* tissues.

BDS I is a peptide toxin with an anti-angiogenic activity from the sea anemone *Anemonia viridis*⁶⁴. APETx1 and APETx2 are peptide toxins with antibacterial and neurotoxic activity from *Anthopleura Elegantissima*. These toxins act on ERG Kv and Nav channels and ASIC3^{56,65–68}. Magnificamide, a peptide inhibitor of mammalian α-amylases, isolated from the venom of sea anemone *Heteractis magnifica*, can be used to control postprandial hyperglycemia in diabetes mellitus⁶⁹. Therefore, its functionally active recombinant analogue is a promising agent that awaits further investigation as a potential drug candidate for the treatment of type 2 diabetes mellitus⁷⁰.

In this study, we identified 11 homologous sequences to sea anemone toxin β-defensin-like peptides with a cysteine pattern of CXC-C-C-CC (Fig. 6a,b). This compact core β-defensin structure relies on disulfide connections formed between cysteines C1-C5, C2-C4, and C3-C6. All these 11 novel homologous sequences were not previously reported. Sequence similarity analysis indicated that the sequence identity of HC-71 and Rc I (GenBank No. P0C5G5.1), HC-66/70 and Am II (GenBank No. P69930.1) was 97.87%, 97.83%, and 95.65%, respectively. Furthermore, HC-64/73 showed high similarities with previously reported sequences (GenBank

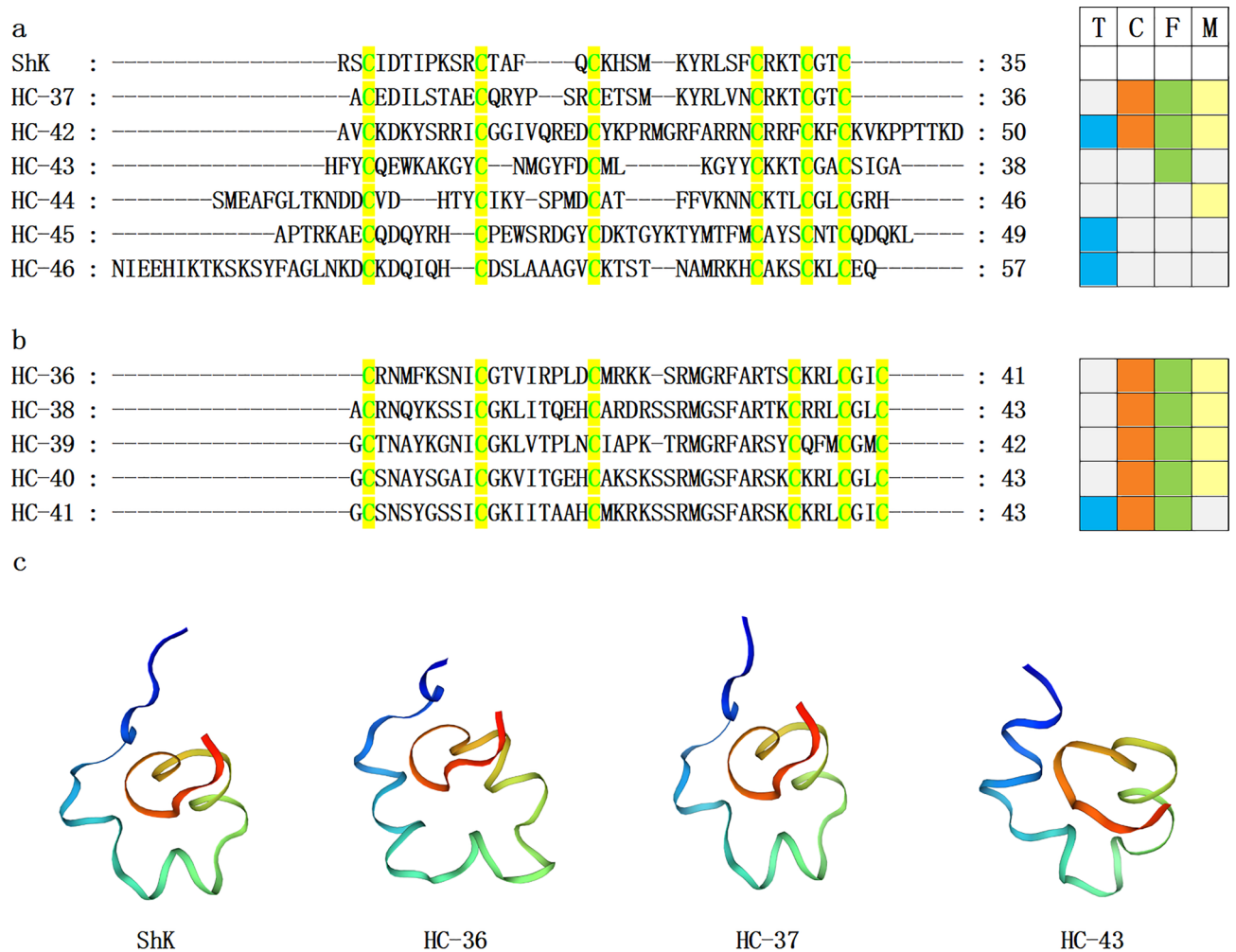


Figure 5. Sea anemone ShKT domain mature peptide sequences. (a–b) The conserved cysteine residues are highlighted with green text on yellow background. T, C, F, and M respectively represent tentacles, column, mesenterial filaments, and combine, highlighted in blue, orange, green, and yellow. (c) Homology modeling and ShK prediction of sea anemone mature peptides HC-36, HC-37, and HC-43 (PDB 4LFQ).

Kazal-like belongs to serine protease inhibitor family and plays crucial roles in host physiological blood coagulation^{91,92}, development regulation, and immunological functions⁹³, in which protease activity is modulated by protease inhibitors⁹⁴. PI-actitoxin-Avd5a is an elastase inhibitor from *Anemonia sulcata*, a 'non-classical' Kazal-type protein, and PI-actitoxin-Avd5a reveals strong inhibition against *Streptomyces griseus* protease B (SGPB)^{95,96}. Taking PI-actitoxin-Avd5a (PDB 1Y1B) as a template for homology modeling, PI-actitoxin-Avd5a and HC-56 revealed similar 3D structures. Accordingly, HC-56 could strongly inhibit SGPB as PI-actitoxin-Avd5a.

ICK is a family of structural peptides that exerts its effects by targeting ion channels and serving as a defense mechanism against pathogens⁹⁷. ICK is found abundantly in various species, and ICK toxins are also prevalent in animal venom that contribute to predation and defense^{97,98}. BcsTx3, an ICK representative, is a Kv channel blocker from *Bunodosoma caissarum*. BcsTx3 mainly inhibits Kv channels, including but unlimited to Kv1.1, rKv1.2, hKv1.3, and rKv1.6. It also paralyzes swimming crabs when injected at the junction between the body and the walking leg⁹⁹. Using blast alignment, the similarity between HC-87 and BcsTx3 (GenBank No.C0HJC4.1) sequences is as high as 72%. BcsTx3 and HC-87 have the same cysteine pattern (C-C-CC-C-C-C-C) (Fig. 8a). Therefore, it can be deduced that HC-87 may have one or all activities of BcsTx3.

MS 9.1, a positive modulator of mammalian TRPA1, is a typical representative of the BBH family⁴¹. TRPA1 is a non-selective cation channel involved in various physiological processes and exhibits significant anti-inflammatory and analgesic activities^{15,100–102}. The homologous alignment results showed that HC-18 was the same as the sequence (GenBank No. BAS68532.1) from sea anemone *Heteractis aurora*. The similarity of HC-18/19 was 87.5%, and they share the same cysteine pattern. The HC-18/19 compounds that have been identified belong to the BBH family. It is hypothesized that the target of these compounds is TRPA1, providing a basis for developing drug screening assays aimed at identifying potential anti-inflammatory and analgesic medications.

Acrorhagin Ic obtained from red waratah sea anemone *Actinia tenebrosa* in New Zealand and Australian, is a member of the Acrorhagin family. HC-85/86 sequence is highly similar to the previously reported

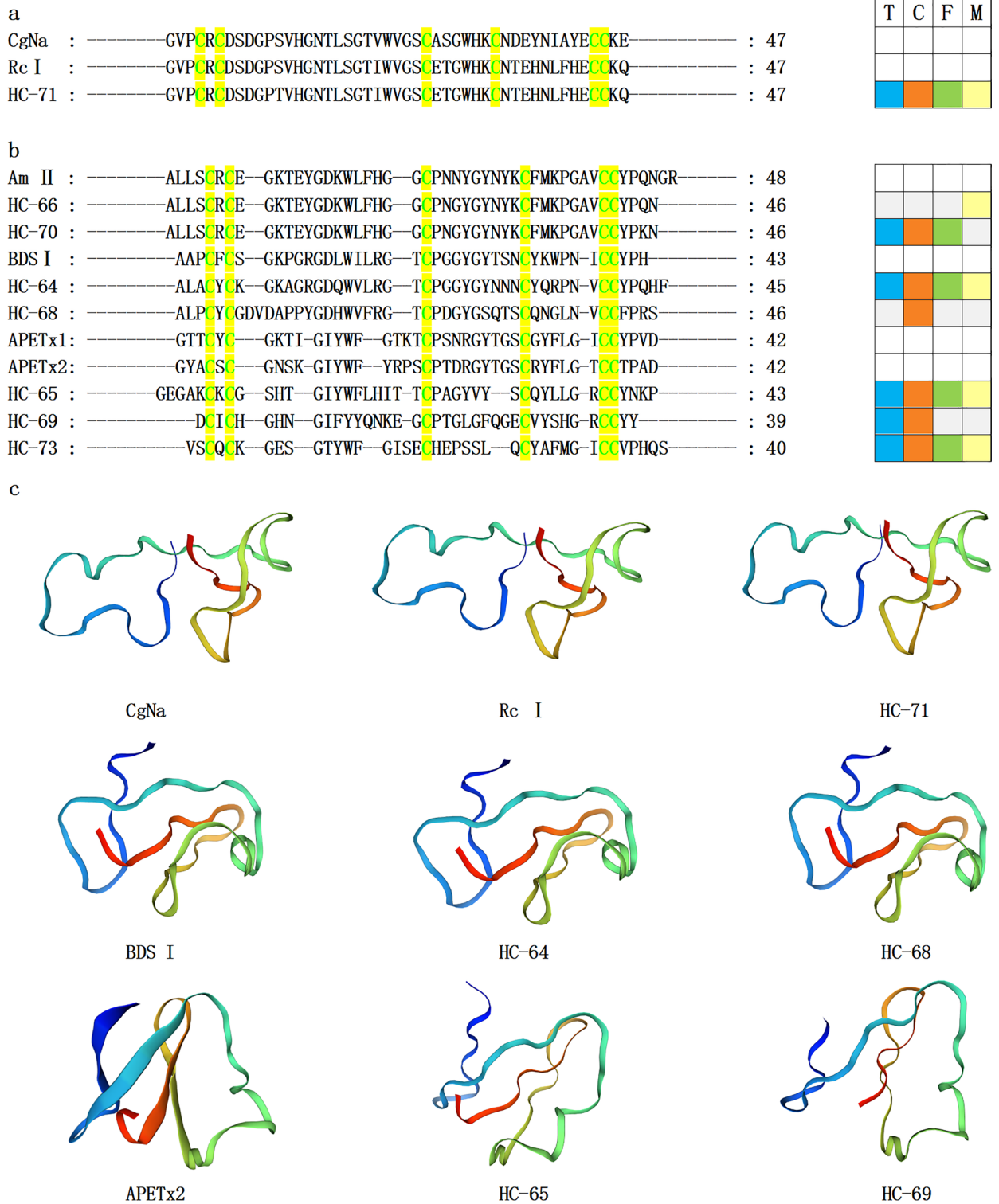


Figure 6. β -defensin-like sea anemone mature peptide sequences. (a–b) The conserved cysteine residues are highlighted with green text on yellow background. T, C, F, and M respectively represent tentacles, column, mesenterial filaments, and combine, highlighted in blue, orange, green, and yellow. (c) Homology modeling prediction of several mature peptides from sea anemones with CgNa (PDB 2H9X), BDS I (PDB 1BDS), and APETx2 (PDB 2MUB).

Acrorhagin Ic sequence (GenBank No. ATY39990.1), and the sequence identity is 61.90% and 59.52%, respectively. Although HC-85/86 and Acrorhagin Ic have similar 3D structures, Acrorhagin Ic is a toxin lethal to crabs

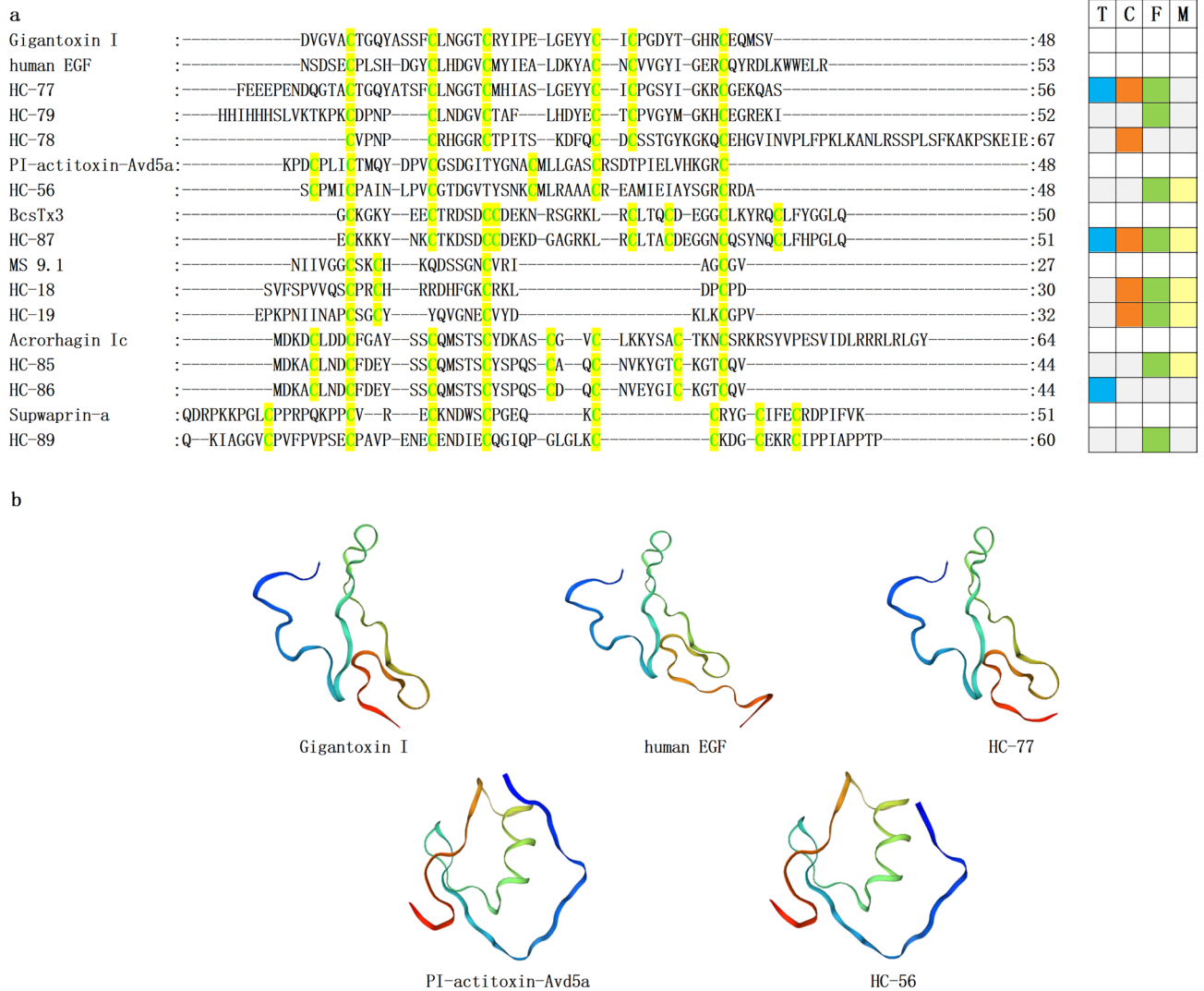


Figure 8. Representative Sea anemone mature peptide sequences in other families. (a) The conserved cysteine residues are highlighted with green text on yellow background. T, C, F, and M respectively represent tentacles, column, mesenterial filaments, and combine, highlighted in blue, orange, green, and yellow. (b) Homology modeling prediction of several representative sea anemone mature peptides with human EGF (PDB 7SZ1), PI-actitoxin-Avd5a (PDB 1Y1B).

peptide components in crude venom of sea anemone *H. crispa*, predict its family classification, and 3D structural and functional annotation.

Three sea anemone *H. crispa* tissues were sequenced and analyzed to explore peptide toxin distribution. Our HTS analysis detected 1049 transcripts, including 416, 291, and 307 putative protein and peptide toxin transcripts, respectively, from the tentacles, column, and mesenterial filaments. Whether these putative protein and peptide toxins are present in the venom needs to be further verified through technologies such as proteomics. Using the combined proteomic and transcriptomic techniques, a holistic overview of the venom arsenal of the well-studied sea anemone was obtained³². Macrander et al³⁰, analyzed three sea anemone *H. crispa* tissues, including the tentacles, column, and filament, obtaining 840 protein and peptide toxins, and the toxin expression levels in the tentacles were significantly higher than those in the column and filament. However, we found that the protein and peptide families of the top 10 TPM sequences in the three tissues are similar, with the overall expression levels of all toxins being highest in the column of sea anemone *H. crispa*, followed by the tentacles and mesenterial filaments. Through comparative analysis, we found that there were significant differences between individuals even within the same species of sea anemone, and determining organizational boundaries may affect the data results. Among the 1049 protein and peptide sequences identified in this study, 88 sequences had a similarity of over 80% with the 840 sequences identified by Jason Macrander³⁰. Among these 88 sequences, the main families of protein toxins are metalloproteinase and protein inhibitor, and the family of peptides is β -defensins and Kunitz-type (Figure S7a). However, a comparative analysis of 93 peptide sequences with previous study data revealed that only 22 sequences shared a similarity of over 80% (Figure S7b). Therefore, using our peptide screening principle, only 208 peptides were screened from 840 sequences identified by Jason Macrander³⁰. Comparative analysis of cysteine in peptides showed that in previous studies, 142 peptides had cysteine residues

wound healing, are widely present in vertebrates, and are one of the main components of the innate immune system^{51–53,118}. β -defensin peptides showed paralytic activity in crustaceans, indicating that it had evolved into a weapon to capture prey¹¹⁹. Here, β -defensin-like peptides are not highly expressed in the tentacles and may have other biological functions.

The most common and pharmacologically valuable peptides in sea anemones are the ShKT domain, β -defensin-like, Kunitz-type, and EGF-like peptides, and they influence various ion channels, including Nav channels, Kv channels, ASIC, TRPV1, and TRPA1^{29,43–45}. The ShKT domain is one of the families with the highest presence in the transcriptome data of sea anemone *H. crispa*, suggesting that this type of peptide toxin may play a crucial role in its predation, defense, and competition^{17,47,48}. ShK inhibits Kv channels, blocking Kv1.1/1.2/1.3/1.6/3.2 and Kca3.1 channels, especially in Kv1.1/KCNA1 and Kv1.3/KCNA3 channels^{16,49,50}. Kv1.3 is involved in various autoimmune diseases and many cancers by contributing to cell proliferation, malignant angiogenesis, and metastasis^{18,20,120–125}. ShK is a Kv1.3 channel blocker analogue with significant roles in T and B lymphocyte subsets related to autoimmune conditions. Therefore, ShK is a potential immune modulator for autoimmune disease therapy⁴⁶. Of these, ShK-186, also known as Dalazatide, was the first representative of the ShKT domain to be detected and characterized and the first drug to complete Phase I trials^{17,46,126}. ShK and its analogues, including 11 homologs in the ShKT domain found in this study, may act on Kv1.3, suggesting that they may have significant involvements in treating human autoimmune disorders^{127–129}.

β -defensin-like peptides block ligated-gated and voltage-gated ion channels, as Nav types 1/2/4, Kv type 3, and ASIC^{54–57,130}. Eleven identified β -defensin-like homologous sequences may act on Nav types 1/2/4 channels related to acute and chronic pain, and it can potentially treat pain^{131,132}. Additionally, these peptides acting on Nav channels, considered insecticidal lead compounds, have insecticidal effects¹³³. Kunitz-type peptides block ion channels and are anti-inflammatory⁷³. HCRG1/2 are the first Kunitz-type peptides to block Kv1.3 found in sea anemones^{27,134}. The first Kunitz-type representative bovine pancreatic trypsin inhibitor (BPTI) is a serine protease inhibitor resisting inflammatory responses^{135,136}. In sea anemones, Kunitz-type peptides act on TRPV1 and Kv channels^{29,74,75}, indirect TRPV1 activation contributes to EGF receptor/PLA2/arachidonic acid/lipoxygenase pathway, resulting in Kunitz-type peptides regulating TRPV1 channel activity^{41,137}. APHC1-3 is earlier shown to possess a unique property of inhibiting of the pain vanilloid receptor TRPV1 in vitro and providing the analgesic effects in vivo in addition to their trypsin inhibitory activity⁷⁶. The activated ion channel TRPV1 produces pain, so TRPV1 is the most important therapeutic target for pain and inflammatory stimulation^{14,29,75,138}. Besides blocking TRPV1 channels, various anemone Kv channel toxins inhibit serine protease activity, participating in various functions, like blood clotting, tumor immunity, fibrinolysis, inflammatory modulation, and resistance against bacterial and fungal infections^{73,139,140}. Seven homologous Kunitz-type peptide sequences were identified, contributing to the anti-inflammatory responses by inhibiting serine protease activity and Kv channels.

The phylogenetic tree of typical family sea anemone peptides exhibited a pattern in which the majority of the sequences were clustered based on families, while a subset of individual sequences remained dispersed among alternative family groupings. The peptide sequence families of the transcriptomes in this study were based on changes in cysteine patterns and 3D structures, resulting in some sequences not being clustered together. Therefore, 3D structural alignment is a very powerful tool for inferring the evolutionary relationship between two low homology peptides.

Conclusions

The transcriptome analysis of *H. crispa* sea anemone venom from the tentacles, column, and mesenterial filaments was performed using HTS technology. A total of 1049 putative protein toxins were obtained, including 956 (91.0%) protein sequences and 93 (9.0%) peptide toxin sequences, which were divided into 60 known families. ShKT domain in peptide toxins was predominantly expressed in the tentacles, column, and mesenterial filaments and contributes to prey capture, defines, and intraspecific competition. Our study demonstrated that the venom assemblages within these different sea anemone *H. crispa* tissues are complex and diverse. Combining HTS and bioinformatics technologies new peptides can be systematically identified in addition to predicting their family categorization, 3D structures, and functional annotations. These advances lay the foundation for enhanced understanding and development of sea anemone venom as potential marine pharmaceuticals.

Materials and methods

Specimens and RNA extraction

The sea anemone was collected from Paracel Islands located at [Lat 15°46' N, Lon 111°11' E] in the Southern Sea of China and maintained in the lab in aquariums containing artificial seawater. The sea anemone sample was identified by the mitochondrial genome as *H. crispa*. A total of three *H. crispa* were collected, and over a week, different tissues were removed from *H. crispa* using tweezers and a scalpel, starting with the tentacles, column, and mesenterial filaments including the pharynx and gonads. Three different *H. crispa* tissue samples were mixed separately, and then the total RNA from these three tissues were extracted after liquid nitrogen flash evaporation (TIANGEN biotech Co., Ltd., China), and their RNA integrity number values were measured using an Agilent 2100 Bioanalyzer (Agilent Tech., Palo Alto, CA, USA). Then, BGI-Tech (Shenzhen, Guangdong, China) was used to build three Illumina cDNA libraries from qualifying RNAs and sequenced them using an Illumina HiSeq4000 platform (San Diego, CA, USA).

Sequence analyses and assembly

This study evaluated the assembly integrity of four assembled transcripts using BUSCO v5.2.2 software and databases: etazoan_Odb10 (Creation date: 2021-02-17, genomes: 65, number of BUSCOs: 954). BUSCO was run in mode: transcriptome. Illumina HTS, raw image data, was converted into raw reads after base calling by

Illumina CASAVA software (v1.8.4). High-quality clean reads were obtained by removing the adapter and reads with > 10% of non-sequenced bases or > 50% of low-quality bases (≤ 10 was the base quality score). We compared the transcriptomes after assembly to evaluate the impact of the cleanup step on overall completeness and also conducted a reciprocal BLAST (Basic Local Alignment Search Tool) search of known sea anemone venom genes to determine whether the alternative cleanup strategies would result in a different number of candidate toxin genes. The transcriptome sequence assembly strategy was used to assemble HTS data into transcript sequences through three steps of Inchworm, Chrysalis, and Butterfly^{36,37}. (A) Inchworm: Use Kmer-based assembly strategy to assemble reads into contigs, (B) Chrysalis: Cluster contigs sequences, define components, and align reads back to components to verify correctness, (C) Butterfly: De Bruijn graph-based assembly strategy to assemble components into possible transcripts. This study generated four transcriptome reference sequences for Tentacles, Column, Mesenterial filaments, and their combination (Combine).

Gene annotation

The Unigene gene's coding region was predicted using the translation approach, and possible coding protein sequences were predicted. The resulting protein sequences were cross-referenced against Uniprot and the non-redundant (NR) protein database (<https://blast.ncbi.nlm.nih.gov/Blast.cgi>). The protein coding model was determined by utilizing the coding mode of the alignment with the highest alignment score. Unigene gene annotation was conducted based on NR, Uniprot, KEGG^{141–143}, and KOG (eukaryotic)/COG (prokaryotic) databases.

Cluster heatmap and GO analysis

Differentially expressed genes (DEGs) between two tissues were determined by a Fold Change (FC) of | LogFC | > 2. The gene expression heatmap is plotted using the TPM value and the R language's photomap package (Pretty Heatmaps (Version 1.0.12) method. GO enrichment analysis of DEGs was conducted by using the cluster profiler program¹⁴⁴. Fisher's exact test pvalue or Benjamin's corrected pvalue less than 0.05 was set as the significant enrichment level.

Identification of protein and peptide toxins

Prediction of sea anemone protein and peptide toxins using four datasets, homolog searches, and an ab initio prediction method (tentacles, column, and mesenterial filaments, Combine). The BLAST database was queried for proteins and peptides for sequence similarity prediction. After assembly, the sequences were checked against a local database using BLASTX (with an E-value of $1e-5$). The BLASTX-hit unigenes were used to generate amino acid sequences. According to the BLAST database's superfamily and family classifications, those four datasets were divided into different groups.

Prediction and comparison of 183,198 transcripts of *H. crispa* were completed by using SPM Predictor (length ≤ 200 , hydrophobic $\geq 70\%$), Diamond ATDB database (with an E-value $\leq 1e-8$) and Diamond NR database (with an E-value $\leq 1e-8$). A Python script was developed to trim all of the sea anemone toxin-candidate transcripts to allow only the open-reading frame (ORF) identified by Transdecoder (<http://transdecoder.github.io>).

Classification of protein and peptide toxins superfamilies

Using the BLAST (default setting), predicted sea anemone peptide and protein transcripts were identified. Peptide and protein toxins with the highest resemblance to known superfamilies in the BLAST database were assigned based on cysteine structural scaffold. Those protein and peptide toxins with low similarities (< 75%) were classified into unknown groups.

Alignment and homology modelling

MEGA 7.0.14 software was used to create new protein sequence alignments and perform amino acid alignments on all peptide sequences, where the MUSCLE algorithm was chosen to intelligently align amino acids^{105,106}. Genedoc software was used to export the sequence in FASTA format.

Protein 3D structure was predicted using homology computational structure prediction modeling from amino acid sequences¹⁴⁵. The SWISS-MODEL, available through the Expasy web server or Deep View software (Swiss Pdb-Viewer) were applied. The homologous sequences with high sequence identity were assigned as templates, and then the cartoon mode was used to build the model.

Phylogenetic analyses

Representative peptide sequences from various families of sea anemones were obtained from UniProt and BLAST databases (www.uniprot.org/, <https://blast.ncbi.nlm.nih.gov/>), and they were comparable to those sequences obtained in this study. The mature regions of 93 peptide sequences were aligned using MEGA 7.0.14. A phylogenetic tree was established using the Neighbor-Joining approach (Bootstrap method 1000 and Pairwise deletion 50%).

Human and animal resources

The article does not involve human or animal experiments, and all sea anemones are collected according to the collection permit issued by the China Fisheries Administration.

Data availability

The datasets described are accessible through internet repositories. The repository(s) and accession number(s) can be accessed at the following URL: <https://www.ncbi.nlm.nih.gov/sra/PRJNA893400> (accession: SRX17999840, SRX17999841, and SRX17999842).

Received: 27 November 2023; Accepted: 28 March 2024

Published online: 01 April 2024

References

- Rodríguez, E. *et al.* Hidden among sea anemones: the first comprehensive phylogenetic reconstruction of the order Actiniaria (Cnidaria, Anthozoa, Hexacorallia) reveals a novel group of hexacorals. *PLoS ONE* **9**, e96998. <https://doi.org/10.1371/journal.pone.0096998> (2014).
- Jouiaei, M. *et al.* 2015 Ancient venom systems: A review on cnidaria toxins. *Toxins* **7**(6), 2251–2271 (2015).
- Erwin, D. H. *et al.* The Cambrian conundrum: early divergence and later ecological success in the early history of animals. *Science* **334**, 1091–1097. <https://doi.org/10.1126/science.1206375> (2011).
- Park, E. *et al.* Estimation of divergence times in cnidarian evolution based on mitochondrial protein-coding genes and the fossil record. *Mol. Phylogenet. Evol.* **62**, 329–345. <https://doi.org/10.1016/j.ympev.2011.10.008> (2012).
- David, C. N. *et al.* Evolution of complex structures: Minicollagens shape the cnidarian nematocyst. *Trends. Genet.* **24**, 431–438. <https://doi.org/10.1016/j.tig.2008.07.001> (2008).
- Beckmann, A. & Ozbek, S. The nematocyst: A molecular map of the cnidarian stinging organelle. *Int. J. Dev. Biol.* **56**, 577–582. <https://doi.org/10.1387/ijdb.113472ab> (2012).
- Lotan, A., Fishman, L., Loya, Y. & Zlotkin, E. Delivery of a nematocyst toxin. *Nature* **375**, 456. <https://doi.org/10.1038/375456a0> (1995).
- Columbus-Shenkar, Y. Y. *et al.* Dynamics of venom composition across a complex life cycle. *Elife* **7**, e35014. <https://doi.org/10.7554/eLife.35014> (2018).
- Moran, Y. *et al.* Neurotoxin localization to ectodermal gland cells uncovers an alternative mechanism of venom delivery in sea anemones. *Proc. Biol. Sci.* **279**, 1351–1358. <https://doi.org/10.1098/rspb.2011.1731> (2012).
- Frazaio, B., Vasconcelos, V. & Antunes, A. Sea anemone (Cnidaria, Anthozoa, Actiniaria) toxins: an overview. *Mar. drugs* **10**, 1812–1851. <https://doi.org/10.3390/md10081812> (2012).
- Moran, Y., Gordon, D. & Gurevitz, M. Sea anemone toxins affecting voltage-gated sodium channels—molecular and evolutionary features. *Toxicon* **54**, 1089–1101. <https://doi.org/10.1016/j.toxicon.2009.02.028> (2009).
- Diochot, S. & Lazdunski, M. Sea anemone toxins affecting potassium channels. *Prog. Mol. Subcell. Biol.* **46**, 99–122. https://doi.org/10.1007/978-3-540-87895-7_4 (2009).
- Rodríguez, A. A. *et al.* A novel sea anemone peptide that inhibits acid-sensing ion channels. *Peptides* **53**, 3–12. <https://doi.org/10.1016/j.peptides.2013.06.003> (2014).
- Andreev, Y. A. *et al.* Analgesic compound from sea anemone *Heteractis crispa* is the first polypeptide inhibitor of vanilloid receptor 1 (TRPV1). *J. Biol. Chem.* **283**, 23914–23921. <https://doi.org/10.1074/jbc.M800776200> (2008).
- Logashina, Y. A. *et al.* Peptide from sea anemone metridium senile affects transient receptor potential ankyrin-repeat 1 (TRPA1) function and produces analgesic effect. *J. Biol. Chem.* **292**, 2992–3004. <https://doi.org/10.1074/jbc.M116.757369> (2017).
- Kalman, K. *et al.* ShK-Dap22, a potent Kv1.3-specific immunosuppressive polypeptide. *J. Biol. Chem.* **273**, 32697–32707. <https://doi.org/10.1074/jbc.273.49.32697> (1998).
- Castaneda, O. *et al.* Characterization of a potassium channel toxin from the Caribbean Sea anemone *Stichodactyla helianthus*. *Toxicon* **33**, 603–613. [https://doi.org/10.1016/0041-0101\(95\)00013-c](https://doi.org/10.1016/0041-0101(95)00013-c) (1995).
- Chandy, K. G. & Norton, R. S. Peptide blockers of Kv1.3 channels in T cells as therapeutics for autoimmune disease. *Curr. Opin. Chem. Biol.* **38**, 97–107. <https://doi.org/10.1016/j.cbpa.2017.02.015> (2017).
- Pennington, M. W. *et al.* Development of highly selective Kv1.3-blocking peptides based on the sea anemone peptide ShK. *Mar. Drugs* **13**, 529–542. <https://doi.org/10.3390/md13010529> (2015).
- Beeton, C. *et al.* Kv1.3 channels are a therapeutic target for T cell-mediated autoimmune diseases. *Proc. Natl. Acad. Sci. USA* **103**, 17414–17419. <https://doi.org/10.1073/pnas.0605136103> (2006).
- Tarcha, E. J. *et al.* Safety and pharmacodynamics of dalazatide, a Kv1.3 channel inhibitor, in the treatment of plaque psoriasis: A randomized phase 1b trial. *PLoS One* **12**, e0180762. <https://doi.org/10.1371/journal.pone.0180762> (2017).
- Kashimoto, R. *et al.* Transcriptomes of giant sea anemones from okinawa as a tool for understanding their phylogeny and symbiotic relationships with anemonefish. *Zool. Sci.* **39**, 374–387. <https://doi.org/10.2108/zs210111> (2022).
- Nguyen, H. T. T., Dang, B. T., Glenner, H. & Geffen, A. J. Cophylogenetic analysis of the relationship between anemonefish amphiprion (Perciformes: Pomacentridae) and their symbiotic host anemones (Anthozoa: Actiniaria). *Mar. Biol. Res.* **16**, 117–133. <https://doi.org/10.1080/17451000.2020.1711952> (2020).
- Titus, B. M. *et al.* Phylogenetic relationships among the clownfish-hosting sea anemones. *Mol. Phylogenet. Evol.* **139**, 106526. <https://doi.org/10.1016/j.ympev.2019.106526> (2019).
- Mebs, D. Anemonefish symbiosis: vulnerability and resistance of fish to the toxin of the sea anemone. *Toxicon* **32**, 1059–1068. [https://doi.org/10.1016/0041-0101\(94\)90390-5](https://doi.org/10.1016/0041-0101(94)90390-5) (1994).
- Fedorov, S. *et al.* The anticancer effects of actinoporin RTX-A from the sea anemone *Heteractis crispa* (= *Radianthus macrodactylus*). *Toxicon* **55**, 811–817. <https://doi.org/10.1016/j.toxicon.2009.11.016> (2010).
- Gladkikh, I. *et al.* Kunitz-type peptides from the sea anemone *Heteractis crispa* demonstrate potassium channel blocking and anti-inflammatory activities. *Biomedicines* **8**, 473. <https://doi.org/10.3390/biomedicines8110473> (2020).
- Kalina, R. S. *et al.* New sea anemone toxin RTX-VI selectively modulates voltage-gated sodium channels. *Dokl. Biochem. Biophys.* **495**, 292–295. <https://doi.org/10.1134/S1607672920060071> (2020).
- Monastyrnaya, M. *et al.* Kunitz-type peptide HCRG21 from the sea anemone *Heteractis crispa* is a full antagonist of the TRPV1 receptor. *Mar. Drugs* **14**, 229. <https://doi.org/10.3390/md14120229> (2016).
- Macrander, J., Broe, M. & Daly, M. Tissue-specific venom composition and differential Gene expression in sea anemones. *Genome Biol. Evol.* **8**, 2358–2375. <https://doi.org/10.1093/gbe/evw155> (2016).
- Delgado, A., Benedict, C., Macrander, J. & Daly, M. Never, Ever make an enemy out of an anemone: Transcriptomic comparison of clownfish hosting sea anemone venoms. *Mar. Drugs* **20**, 730. <https://doi.org/10.3390/md20120730> (2022).
- Madio, B., Undheim, E. A. B. & King, G. F. Revisiting venom of the sea anemone *Stichodactyla haddoni*: Omics techniques reveal the complete toxin arsenal of a well-studied sea anemone genus. *J. Proteomics* **166**, 83–92. <https://doi.org/10.1016/j.jprot.2017.07.007> (2017).
- Ramirez-Carreto, S. *et al.* Transcriptomic and proteomic analysis of the tentacles and mucus of *Anthopleura dowii* Verrill, 1869. *Mar. Drugs* **17**, 436. <https://doi.org/10.3390/md17080436> (2019).

34. Rodriguez, A. A. *et al.* Peptide fingerprinting of the neurotoxic fractions isolated from the secretions of sea anemones *Stichodactyla helianthus* and *Bunodosoma granulifera*. New members of the APETx-like family identified by a 454 pyrosequencing approach. *Peptides* **34**, 26–38. <https://doi.org/10.1016/j.peptides.2011.10.011> (2012).
35. Seppely, M., Manni, M. & Zdobnov, E. M. BUSCO: assessing genome assembly and annotation completeness. *Methods Mol. Biol.* **1962**, 227–245. https://doi.org/10.1007/978-1-4939-9173-0_14 (2019).
36. Grabherr, M. G. *et al.* Full-length transcriptome assembly from RNA-Seq data without a reference genome. *Nat. Biotechnol.* **29**, 644–652. <https://doi.org/10.1038/nbt.1883> (2011).
37. Li, B. & Dewey, C. N. RSEM: Accurate transcript quantification from RNA-Seq data with or without a reference genome. *BMC Bioinformatics* **12**, 323. <https://doi.org/10.1186/1471-2105-12-323> (2011).
38. Kozlov, S. & Grishin, E. Convenient nomenclature of cysteine-rich polypeptide toxins from sea anemones. *Peptides* **33**, 240–244. <https://doi.org/10.1016/j.peptides.2011.12.008> (2012).
39. Fu, J., Liao, Y., Jin, A. H. & Gao, B. Discovery of novel peptide neurotoxins from sea anemone species. *Front. Biosci. Landmark* **26**(11), 1256–1273. <https://doi.org/10.52586/5022> (2021).
40. Fu, J. X. *et al.* Transcriptome sequencing of the pale anemones (*Exaiptasia diaphana*) revealed functional peptide gene resources of sea anemone. *Front. Mar. Sci.* **9**, 856501. <https://doi.org/10.3389/fmars.2022.856501> (2022).
41. Madio, B., King, G. F. & Undheim, E. A. B. Sea anemone toxins: a structural overview. *Mar. Drugs* **17**, 325. <https://doi.org/10.3390/md17060325> (2019).
42. Menezes, C. & Thakur, N. L. Sea anemone venom: Ecological interactions and bioactive potential. *Toxicon* **208**, 31–46. <https://doi.org/10.1016/j.toxicon.2022.01.004> (2022).
43. Bosmans, F. & Tytgat, J. Sea anemone venom as a source of insecticidal peptides acting on voltage-gated Na⁺ channels. *Toxicon* **49**, 550–560. <https://doi.org/10.1016/j.toxicon.2006.11.029> (2007).
44. Castañeda, O. & Harvey, A. L. Discovery and characterization of cnidarian peptide toxins that affect neuronal potassium ion channels. *Toxicon* **54**, 1119–1124. <https://doi.org/10.1016/j.toxicon.2009.02.032> (2009).
45. Cristofori-Armstrong, B. & Rash, L. D. Acid-sensing ion channel (ASIC) structure and function: Insights from spider, snake and sea anemone venoms. *Neuropharmacology* **127**, 173–184. <https://doi.org/10.1016/j.neuropharm.2017.04.042> (2017).
46. Pennington, M. W. *et al.* Chemical synthesis and characterization of ShK toxin: a potent potassium channel inhibitor from a sea anemone. *Int. J. Pept. Protein Res.* **46**, 354–358. <https://doi.org/10.1111/j.1399-3011.1995.tb01068.x> (1995).
47. Shafee, T., Mitchell, M. L. & Norton, R. S. Mapping the chemical and sequence space of the ShKT superfamily. *Toxicon* **165**, 95–102. <https://doi.org/10.1016/j.toxicon.2019.04.008> (2019).
48. Krishnarjuna, B. *et al.* Synthesis, folding, structure and activity of a predicted peptide from the sea anemone *Oulactis* sp. with an ShKT fold. *Toxicon* **150**, 50–59. <https://doi.org/10.1016/j.toxicon.2018.05.006> (2018).
49. Rauer, H., Pennington, M., Cahalan, M. & Chandy, K. G. Structural conservation of the pores of calcium-activated and voltage-gated potassium channels determined by a sea anemone toxin. *J. Biol. Chem.* **274**, 21885–21892. <https://doi.org/10.1074/jbc.274.31.21885> (1999).
50. Yan, L. *et al.* Stichodactyla helianthus peptide, a pharmacological tool for studying Kv3.2 channels. *Mol. Pharmacol.* **67**, 1513–1521. <https://doi.org/10.1124/mol.105.011064> (2005).
51. Oguiura, N., Correa, P. G., Rosmino, I. L., de Souza, A. O. & Pasqualoto, K. F. M. Antimicrobial activity of snake beta-defensins and derived peptides. *Toxins Basel* **14**, 1. <https://doi.org/10.3390/toxins14010001> (2021).
52. Shafee, T. M., Lay, F. T., Hulett, M. D. & Anderson, M. A. The defensins consist of two independent, convergent protein super-families. *Mol. Biol. Evol.* **33**, 2345–2356. <https://doi.org/10.1093/molbev/msw106> (2016).
53. Zhu, S. & Gao, B. Evolutionary origin of beta-defensins. *Dev. Comp. Immunol.* **39**, 79–84. <https://doi.org/10.1016/j.dci.2012.02.011> (2013).
54. Cariello, L. *et al.* Calitoxin, a neurotoxic peptide from the sea anemone *Calliactis parasitica*: amino acid sequence and electrophysiological properties. *Biochemistry* **28**, 2484–2489. <https://doi.org/10.1021/bi00432a020> (1989).
55. Ishida, M., Yokoyama, A., Shimakura, K., Nagashima, Y. & Shiomi, K. H. a polypeptide toxin from the sea anemone *Halcurias* sp., with a structural resemblance to type I and 2 toxins. *Toxicon* **35**, 537–544. [https://doi.org/10.1016/s0041-0101\(96\)00143-2](https://doi.org/10.1016/s0041-0101(96)00143-2) (1997).
56. Diochot, S. *et al.* A new sea anemone peptide, APETx2, inhibits ASIC3, a major acid-sensitive channel in sensory neurons. *Embo. j.* **23**, 1516–1525. <https://doi.org/10.1038/sj.emboj.7600177> (2004).
57. Diochot, S., Schweitz, H., Béress, L. & Lazdunski, M. Sea anemone peptides with a specific blocking activity against the fast inactivating potassium channel Kv3.4. *J. Biol. Chem.* **273**, 6744–6749. <https://doi.org/10.1074/jbc.273.12.6744> (1998).
58. Kalina, R. S. *et al.* APETx-like peptides from the sea anemone *Heteractis crispata*, diverse in their effect on ASIC1a and ASIC3 ion channels. *Toxins Basel*. <https://doi.org/10.3390/toxins12040266> (2020).
59. Blanchard, M. G., Rash, L. D. & Kellenberger, S. Inhibition of voltage-gated Na⁺ currents in sensory neurones by the sea anemone toxin APETx2. *Br. J. Pharmacol.* **165**, 2167–2177. <https://doi.org/10.1111/j.1476-5381.2011.01674.x> (2012).
60. Jensen, J. E. *et al.* Cyclisation increases the stability of the sea anemone peptide APETx2 but decreases its activity at acid-sensing ion channel 3. *Mar. Drugs* **10**, 1511–1527. <https://doi.org/10.3390/md10071511> (2012).
61. Salceda, E. *et al.* CgNa, a type I toxin from the giant Caribbean sea anemone *Condylactis gigantea* shows structural similarities to both type I and II toxins, as well as distinctive structural and functional properties(1). *Biochem. J.* **406**, 67–76. <https://doi.org/10.1042/bj20070130> (2007).
62. Shiomi, K., Lin, X. Y., Nagashima, Y. & Ishida, M. Isolation and amino acid sequence of a polypeptide toxin from the sea anemone *Radianthus crispus*. *Fisheries Sci.* **62**, 629–633 (2011).
63. Honma, T. *et al.* Isolation and molecular cloning of novel peptide toxins from the sea anemone *Antheopsis maculata*. *Toxicon* **45**, 33–41. <https://doi.org/10.1016/j.toxicon.2004.09.013> (2005).
64. Loret, E. P. *et al.* A low molecular weight protein from the sea anemone *Anemonia viridis* with an anti-angiogenic activity. *Mar. Drugs* **16**, 134. <https://doi.org/10.3390/md16040134> (2018).
65. Diochot, S., Loret, E., Bruhn, T., Béress, L. & Lazdunski, M. APETx1, a new toxin from the sea anemone *Anthopleura elegantissima*, blocks voltage-gated human ether-a-go-go-related gene potassium channels. *Mol. Pharmacol.* **64**, 59–69. <https://doi.org/10.1124/mol.64.1.59> (2003).
66. Restano-Cassulini, R. *et al.* Species diversity and peptide toxins blocking selectivity of ether-a-go-go-related gene subfamily K⁺ channels in the central nervous system. *Mol. Pharmacol.* **69**, 1673–1683. <https://doi.org/10.1124/mol.105.019729> (2006).
67. Zhang, M., Liu, X. S., Diochot, S., Lazdunski, M. & Tseng, G. N. APETx1 from sea anemone *Anthopleura elegantissima* is a gating modifier peptide toxin of the human ether-a-go-go-related potassium channel. *Mol. Pharmacol.* **72**, 259–268. <https://doi.org/10.1124/mol.107.035840> (2007).
68. Peigneur, S. *et al.* A natural point mutation changes both target selectivity and mechanism of action of sea anemone toxins. *Faseb. J.* **26**, 5141–5151. <https://doi.org/10.1096/fj.12-218479> (2012).
69. Popkova, D. *et al.* Bioprospecting of sea anemones (Cnidaria, Anthozoa, Actiniaria) for β-defensin-like α-amylase inhibitors. *Biomedicines* **11**, 2682. <https://doi.org/10.3390/biomedicines11102682> (2023).
70. Sintsova, O. *et al.* Magnificamide, a β-defensin-like peptide from the mucus of the sea anemone *Heteractis magnifica*, is a strong inhibitor of mammalian α-amylases. *Mar. Drugs* **17**, 542. <https://doi.org/10.3390/md17100542> (2019).

71. Kvetkina, A. *et al.* A new multigene HClQ subfamily from the sea anemone *Heteractis crispa* encodes Kunitz-peptides exhibiting neuroprotective activity against 6-hydroxydopamine. *Sci. Rep.* **10**(1), 4205 (2020).
72. Mourao, C. B. F. & Schwartz, E. F. Protease inhibitors from marine venomous animals and their counterparts in terrestrial venomous animals. *Mar. Drugs* **11**, 2069–2112. <https://doi.org/10.3390/md11062069> (2013).
73. Mishra, M. Evolutionary aspects of the structural convergence and functional diversification of Kunitz-domain inhibitors. *J. Mol. Evol.* **88**, 537–548. <https://doi.org/10.1007/s00239-020-09959-9> (2020).
74. Hwang, S. M. *et al.* Venom peptide toxins targeting the outer pore region of transient receptor potential vanilloid 1 in pain: implications for analgesic drug development. *Int. J. Mol. Sci.* **23**, 5772. <https://doi.org/10.3390/ijms23105772> (2022).
75. Sintsova, O. V. *et al.* Peptide blocker of ion channel TRPV1 exhibits a long analgesic effect in the heat stimulation model. *Dokl. Biochem. Biophys.* **493**, 215–217. <https://doi.org/10.1134/S1607672920030096> (2020).
76. Zelepuga, E. A. *et al.* Interaction of sea anemone *Heteractis crispa* Kunitz type polypeptides with pain vanilloid receptor TRPV1: in silico investigation. *Bioorg. Khim.* **38**, 185–198. <https://doi.org/10.1134/s106816201202015x> (2012).
77. Schweitz, H. *et al.* Kalicicludines and kaliseptine. Two different classes of sea anemone toxins for voltage sensitive K⁺ channels. *J. Biol. Chem.* **270**, 25121–25126. <https://doi.org/10.1074/jbc.270.42.25121> (1995).
78. Garcia-Fernandez, R. *et al.* The Kunitz-type protein ShPI-1 inhibits serine proteases and voltage-gated potassium channels. *Toxins Basel* **8**, 110. <https://doi.org/10.3390/toxins8040110> (2016).
79. García-Fernández, R. *et al.* Two variants of the major serine protease inhibitor from the sea anemone *Stichodactyla helianthus*, expressed in *Pichia pastoris*. *Protein. Expr. Purif.* **123**, 42–50. <https://doi.org/10.1016/j.pep.2016.03.003> (2016).
80. García-Fernández, R. *et al.* Structure of the recombinant BPTI/Kunitz-type inhibitor rShPI-1A from the marine invertebrate *Stichodactyla helianthus*. *Acta Crystallogr. Sect. F Struct. Biol. Cryst. Commun.* **68**, 1289–1293. <https://doi.org/10.1107/s1744309112039085> (2012).
81. Garcia-Fernandez, R. *et al.* Structural insights into serine protease inhibition by a marine invertebrate BPTI Kunitz-type inhibitor. *J. Struct. Biol.* **180**, 271–279. <https://doi.org/10.1016/j.jsb.2012.08.009> (2012).
82. Tokunaga, A. *et al.* Clinical significance of epidermal growth factor (EGF), EGF receptor, and c-erbB-2 in human gastric cancer. *Cancer* **75**, 1418–1425. [https://doi.org/10.1002/1097-0142\(19950315\)75:6+%3c1418::aid-cnrcr2820751505%3e3.0.co;2-y](https://doi.org/10.1002/1097-0142(19950315)75:6+%3c1418::aid-cnrcr2820751505%3e3.0.co;2-y) (1995).
83. Maruo, T., Matsuo, H., Otani, T. & Mochizuki, M. Role of epidermal growth factor (EGF) and its receptor in the development of the human placenta. *Reprod. Fertil. Dev.* **7**, 1465–1470. <https://doi.org/10.1071/rd9951465> (1995).
84. Normanno, N., Bianco, C., De Luca, A. & Salomon, D. S. The role of EGF-related peptides in tumor growth. *Front. Biosci.* **6**, D685–707. <https://doi.org/10.2741/normano> (2001).
85. De Luca, A. *et al.* EGF-related peptides are involved in the proliferation and survival of MDA-MB-468 human breast carcinoma cells. *Int. J. Cancer* **80**, 589–594. [https://doi.org/10.1002/\(sici\)1097-0215\(19990209\)80:4%3c589::aid-ijc17%3e3.0.co;2-d](https://doi.org/10.1002/(sici)1097-0215(19990209)80:4%3c589::aid-ijc17%3e3.0.co;2-d) (1999).
86. Masilamani, A. P. *et al.* Epidermal growth factor based targeted toxin for the treatment of bladder cancer. *Anticancer Res.* **41**(8), 3741–3746. <https://doi.org/10.21873/anticancer.15165> (2021).
87. Tokay, E. Epidermal growth factor mediates up-regulation of URGCP oncogene in human hepatoma cancer cells. *Mol. Biol. Mosk* **55**, 676–682. <https://doi.org/10.31857/S0026898421040133> (2021).
88. Hermann, P. M., Schein, C. H., Nagle, G. T. & Wildering, W. C. Lymnaea EGF and gigantoxin I, novel invertebrate members of the epidermal growth factor family. *Curr. Pharm. Des.* **10**, 3885–3892. <https://doi.org/10.2174/1381612043382503> (2004).
89. Shiomi, K. *et al.* An epidermal growth factor-like toxin and two sodium channel toxins from the sea anemone *Stichodactyla gigantea*. *Toxicon* **41**, 229–236. [https://doi.org/10.1016/s0041-0101\(02\)00281-7](https://doi.org/10.1016/s0041-0101(02)00281-7) (2003).
90. Honma, T. & Shiomi, K. Peptide toxins in sea anemones: Structural and functional aspects. *Mar. Biotechnol. NY* **8**, 1–10. <https://doi.org/10.1007/s10126-005-5093-2> (2006).
91. Meiser, C. K. *et al.* K26L-type inhibitors in the stomach of *Panstrongylus megistus* (Triatominae, Reduviidae). *Insect. Biochem. Mol. Biol.* **40**, 345–353. <https://doi.org/10.1016/j.ibmb.2010.02.011> (2010).
92. Lovato, D. V., Nicolau de Campos, I. T., Amino, R. & Tanaka, A. S. The full-length cDNA of anticoagulant protein infestin revealed a novel releasable Kazal domain, a neutrophil elastase inhibitor lacking anticoagulant activity. *Biochimie* **88**, 673–681. <https://doi.org/10.1016/j.biochi.2005.11.011> (2006).
93. Soto, A. *et al.* Contribution of kazal-like domains of the serine protease inhibitor-1 from *Toxoplasma gondii* in asthma therapeutic vaccination effectiveness. *Int. Arch. Allergy Immunol.* **183**, 471–478. <https://doi.org/10.1159/000520796> (2022).
94. van Hoef, V. *et al.* Phylogenetic distribution of protease inhibitors of the Kazal-family within the Arthropoda. *Peptides* **41**, 59–65. <https://doi.org/10.1016/j.peptides.2012.10.015> (2013).
95. Hemmi, H. *et al.* Structural and functional study of an *Anemonia sulcata* elastase inhibitor, a “nonclassical” Kazal-type inhibitor from *Anemonia sulcata*. *Biochemistry* **44**, 9626–9636. <https://doi.org/10.1021/bi0472806> (2005).
96. Zheng, Q. L., Sheng, Q. & Zhang, Y. Z. Progresses in the structure and function of Kazal-type proteinase inhibitors. *Sheng Wu Gong Cheng Xue Bao* **22**, 695–700 (2006).
97. Meissner, G. O. *et al.* Molecular cloning and in silico characterization of knottin peptide, U2-SCRTX-Lit2, from brown spider (*Loxosceles intermedia*) venom glands. *J. Mol. Model.* **22**, 196. <https://doi.org/10.1007/s00894-016-3067-0> (2016).
98. Matsubara, F. H. *et al.* A novel ICK peptide from the *Loxosceles intermedia* (brown spider) venom gland: cloning, heterologous expression and immunological cross-reactivity approaches. *Toxicon* **71**, 147–158. <https://doi.org/10.1016/j.toxicon.2013.05.014> (2013).
99. Orts, D. J. *et al.* BcsTx3 is a founder of a novel sea anemone toxin family of potassium channel blocker. *FEBS J.* **280**, 4839–4852. <https://doi.org/10.1111/febs.12456> (2013).
100. Logashina, Y. A. *et al.* Analysis of structural determinants of peptide MS 9a–1 essential for potentiating of TRPA1 channel. *Mar. Drugs* **20**, 465. <https://doi.org/10.3390/md20070465> (2022).
101. Beskhmel'nitsyna, E. A., Pokrovskii, M. V., Kulikov, A. L., Peresypkina, A. A. & Varavin, E. I. Study of anti-inflammatory activity of a new non-opioid analgesic on the basis of a selective inhibitor of TRPA1 ion channels. *Antiinflamm. Antiallergy Agents Med. Chem.* **18**, 110–125. <https://doi.org/10.2174/1871523018666190208123700> (2019).
102. Logashina, Y. A. *et al.* Anti-inflammatory and analgesic effects of TRPV1 polypeptide modulator APHC3 in models of osteo- and Rheumatoid Arthritis. *Mar. Drugs* <https://doi.org/10.3390/md19010039> (2021).
103. Honma, T. *et al.* Novel peptide toxins from acrorhagi, aggressive organs of the sea anemone *Actinia equina*. *Toxicon* **46**, 768–774. <https://doi.org/10.1016/j.toxicon.2005.08.003> (2005).
104. Krishnarajuna, B. *et al.* A disulfide-stabilised helical hairpin fold in acrorhagin I: An emerging structural motif in peptide toxins. *J. Struct. Biol.* **213**, 107692. <https://doi.org/10.1016/j.jsb.2020.107692> (2021).
105. Kumar, S., Stecher, G. & Tamura, K. MEGA7: molecular evolutionary genetics analysis version 7.0 for bigger datasets. *Mol. Biol. Evol.* **33**, 1870–1874. <https://doi.org/10.1093/molbev/msw054> (2016).
106. Hall, B. G. Building phylogenetic trees from molecular data with MEGA. *Mol. Biol. Evol.* **30**, 1229–1235. <https://doi.org/10.1093/molbev/mst012> (2013).
107. Warner, J. F. & Röttinger, E. Transcriptomic analysis in the sea anemone *Nematostella vectensis*. *Methods Mol. Biol.* **2219**, 231–240. https://doi.org/10.1007/978-1-0716-0974-3_14 (2021).
108. Mitchell, M. L. *et al.* Identification, synthesis, conformation and activity of an insulin-like peptide from a sea anemone. *Biomolecules* **11**, 1785. <https://doi.org/10.3390/biom11121785> (2021).

109. Mitchell, M. L. *et al.* Tentacle transcriptomes of the speckled anemone (Actiniaria: Actiniidae: Oulactis sp.): Venom-related components and their domain structure. *Mar. Biotechnol.* **22**, 207–219. <https://doi.org/10.1007/s10126-020-09945-8> (2020).
110. Krishnarjuna, B. *et al.* Structure, folding and stability of a minimal homologue from *Anemonia sulcata* of the sea anemone potassium channel blocker ShK. *Peptides* **99**, 169–178. <https://doi.org/10.1016/j.peptides.2017.10.001> (2018).
111. Macrander, J., Brugler, M. R. & Daly, M. A RNA-seq approach to identify putative toxins from acrorhagi in aggressive and non-aggressive *Anthopleura elegantissima* polyps. *BMC Genomics* **16**, 221. <https://doi.org/10.1186/s12864-015-1417-4> (2015).
112. Davey, P. A., Rodrigues, M., Clarke, J. L. & Aldred, N. Transcriptional characterisation of the *Exaiptasia pallida* pedal disc. *BMC Genomics* **20**, 581. <https://doi.org/10.1186/s12864-019-5917-5> (2019).
113. Graftskaia, E. N. *et al.* Discovery of novel antimicrobial peptides: A transcriptomic study of the sea anemone *Cnidopus japonicus*. *J. Bioinform. Comput. Biol.* **16**, 1840006. <https://doi.org/10.1142/s0219720018400061> (2018).
114. Kvetkina, A. *et al.* Sea anemone *Heteractis crispa* actinoporin demonstrates in vitro anticancer activities and prevents HT-29 colorectal cancer cell migration. *Molecules* **25**, 5979. <https://doi.org/10.3390/molecules25245979> (2020).
115. Yan, L., Leontovich, A., Fei, K. & Sarras, M. P. Jr. Hydra metalloproteinase 1: A secreted astacin metalloproteinase whose apical axis expression is differentially regulated during head regeneration. *Dev. Biol.* **219**, 115–128. <https://doi.org/10.1006/dbio.1999.9568> (2000).
116. Pan, T., Gröger, H., Schmid, V. & Spring, J. A toxin homology domain in an astacin-like metalloproteinase of the jellyfish *Podocoryne carnea* with a dual role in digestion and development. *Dev. Genes. Evol.* **208**, 259–266. <https://doi.org/10.1007/s004270050180> (1998).
117. Surm, J. M. *et al.* A process of convergent amplification and tissue-specific expression dominates the evolution of toxin and toxin-like genes in sea anemones. *Mol. Ecol.* **28**, 2272–2289. <https://doi.org/10.1111/mec.15084> (2019).
118. Stewart, Z. K., Pavasovic, A., Hock, D. H. & Prentis, P. J. Transcriptomic investigation of wound healing and regeneration in the cnidarian *Calliactis polypus*. *Sci. Rep.* **7**, 41458. <https://doi.org/10.1038/srep41458> (2017).
119. Kim, C. H. *et al.* Defensin-neurotoxin dyad in a basally branching metazoan sea anemone. *FEBS J.* **284**, 3320–3338. <https://doi.org/10.1111/febs.14194> (2017).
120. Gubic, S. *et al.* Discovery of K(V)13 ion channel inhibitors: Medicinal chemistry approaches and challenges. *Med. Res. Rev.* **41**, 2423–2473. <https://doi.org/10.1002/med.21800> (2021).
121. Chandy, K. G. *et al.* K⁺ channels as targets for specific immunomodulation. *Trends Pharmacol. Sci.* **25**, 280–289. <https://doi.org/10.1016/j.tips.2004.03.010> (2004).
122. Feske, S., Skolnik, E. Y. & Prakriya, M. Ion channels and transporters in lymphocyte function and immunity. *Nat. Rev. Immunol.* **12**, 532–547. <https://doi.org/10.1038/nri3233> (2012).
123. Pardo, L. A. & Stühmer, W. The roles of K(+) channels in cancer. *Nat. Rev. Cancer* **14**, 39–48. <https://doi.org/10.1038/nrc3635> (2014).
124. Chandy, K. G. & Norton, R. S. Immunology: Channelling potassium to fight cancer. *Nature* **537**, 497–499. <https://doi.org/10.1038/nature19467> (2016).
125. Teisseyre, A., Palko-Labuz, A., Sroda-Pomianek, K. & Michalak, K. Voltage-gated potassium channel Kv1.3 as a target in therapy of cancer. *Front. Oncol.* **9**, 933. <https://doi.org/10.3389/fonc.2019.00933> (2019).
126. Prentis, P. J., Pavasovic, A. & Norton, R. S. Sea anemones: Quiet achievers in the field of peptide toxins. *Toxins Basel* <https://doi.org/10.3390/toxins10010036> (2018).
127. Norton, R. S., Pennington, M. W. & Wulff, H. Potassium channel blockade by the sea anemone toxin ShK for the treatment of multiple sclerosis and other autoimmune diseases. *Curr. Med. Chem.* **11**, 3041–3052. <https://doi.org/10.2174/0929867043633947> (2004).
128. Chi, V. *et al.* Development of a sea anemone toxin as an immunomodulator for therapy of autoimmune diseases. *Toxicon* **59**, 529–546. <https://doi.org/10.1016/j.toxicon.2011.07.016> (2012).
129. Beeton, C., Pennington, M. W. & Norton, R. S. Analogs of the sea anemone potassium channel blocker ShK for the treatment of autoimmune diseases. *Inflamm. Allergy Drug Targets* **10**, 313–321. <https://doi.org/10.2174/187152811797200641> (2011).
130. Matsumura, K. *et al.* Mechanism of hERG inhibition by gating-modifier toxin, APETx1, deduced by functional characterization. *BMC Mol. Cell. Biol.* **22**, 3. <https://doi.org/10.1186/s12860-020-00337-3> (2021).
131. Bagal, S. K., Marron, B. E., Owen, R. M., Storer, R. I. & Swain, N. A. Voltage gated sodium channels as drug discovery targets. *Channels* **9**, 360–366. <https://doi.org/10.1080/19336950.2015.1079674> (2015).
132. Cardoso, F. C. & Lewis, R. J. Sodium channels and pain: From toxins to therapies. *Brit. J. Pharmacol.* **175**, 2138–2157. <https://doi.org/10.1111/bph.13962> (2018).
133. Bosmans, F. & Tytgat, J. Voltage-gated sodium channel modulation by scorpion alpha-toxins. *Toxicon* **49**, 142–158. <https://doi.org/10.1016/j.toxicon.2006.09.023> (2007).
134. Gladkikh, I. *et al.* New Kunitz-type HCRG polypeptides from the sea anemone *Heteractis crispa*. *Mar. Drugs* **13**, 6038–6063. <https://doi.org/10.3390/md13106038> (2015).
135. Kunitz, M. & Northrop, J. H. Isolation from beef pancreas of crystalline trypsinogen, Trypsin, a trypsin inhibitor, and an inhibitor-trypsin compound. *J. Gen. Physiol.* **19**, 991–1007. <https://doi.org/10.1085/jgp.19.6.991> (1936).
136. Ascenzi, P. *et al.* The bovine basic pancreatic trypsin inhibitor (Kunitz inhibitor): a milestone protein. *Curr. Protein Pept. Sci.* **4**, 231–251. <https://doi.org/10.2174/1389203033487180> (2003).
137. Cuypers, E., Peigneur, S., Debaveye, S., Shiomi, K. & Tytgat, J. TRPV1 channel as new target for marine toxins: Example of gigantoxin I, a sea anemone toxin acting via modulation of the PLA2 pathway. *Acta Chim. Slov.* **58**, 735–741 (2011).
138. Hu, B. *et al.* Purification and characterization of gigantoxin-4, a new actinoporin from the sea anemone *Stichodactyla gigantea*. *Int. J. Biol. Sci.* **7**, 729–739. <https://doi.org/10.7150/ijbs.7.729> (2011).
139. Liu, Y., Jiang, S., Li, Q. & Kong, Y. Advances of Kunitz-type serine protease inhibitors. *Sheng Wu Gong Cheng Xue Bao* **37**, 3988–4000. <https://doi.org/10.13345/j.cjb.200802> (2021).
140. Honma, T. *et al.* Novel peptide toxins from the sea anemone *Stichodactyla haddoni*. *Peptides* **29**, 536–544. <https://doi.org/10.1016/j.peptides.2007.12.010> (2008).
141. Kanehisa, M., Furumichi, M., Sato, Y., Kawashima, M. & Ishiguro-Watanabe, M. KEGG for taxonomy-based analysis of pathways and genomes. *Nucl. Acids Res.* **51**, D587–d592. <https://doi.org/10.1093/nar/gkac963> (2023).
142. Kanehisa, M. Toward understanding the origin and evolution of cellular organisms. *Protein Sci.* **28**, 1947–1951. <https://doi.org/10.1002/pro.3715> (2019).
143. Kanehisa, M. & Goto, S. KEGG: Kyoto encyclopedia of genes and genomes. *Nucleic Acids Res.* **28**, 27–30. <https://doi.org/10.1093/nar/28.1.27> (2000).
144. Yu, G. C., Wang, L. G., Han, Y. Y. & He, Q. Y. clusterProfiler: An R package for comparing biological themes among gene clusters. *Omic* **16**, 284–287. <https://doi.org/10.1089/omi.2011.0118> (2012).
145. Muhammed, M. T. & Aki-Yalcin, E. Homology modeling in drug discovery: Overview, current applications, and future perspectives. *Chem. Biol. Drug Des.* **93**, 12–20. <https://doi.org/10.1111/cbdd.13388> (2019).

Author contributions

Bingmiao Gao and Junqing Zhang were responsible for the conception and design of the project. Qiqi Guo, Jinxing Fu, Yanling Liao, and Lin Yuan performed data analysis. The first draft of the manuscript was written by Qiqi Guo and Bingmiao Gao. Ming Li, Xinzhong Li, and Bo Yi revised the manuscript. All authors reviewed the manuscript.

Funding

This work was funded by the Chinese National Natural Science Foundation (no. 82060686), Hainan Province Health Industry Research Project (22A200358), special scientific research project of Hainan academician innovation platform (YSPTZX202132), Hainan Provincial Key Point Research and Invention Program (ZDYF-2022SHFZ309), Hainan Provincial Natural Science Foundation (no. 820RC636) and Hainan Medical University graduate innovation and entrepreneurship training program (no. HYY52021A24).

Competing interests

The authors declare no competing interests.

Additional information

Supplementary Information The online version contains supplementary material available at <https://doi.org/10.1038/s41598-024-58402-2>.

Correspondence and requests for materials should be addressed to J.Z. or B.G.

Reprints and permissions information is available at www.nature.com/reprints.

Publisher's note Springer Nature remains neutral with regard to jurisdictional claims in published maps and institutional affiliations.



Open Access This article is licensed under a Creative Commons Attribution 4.0 International License, which permits use, sharing, adaptation, distribution and reproduction in any medium or format, as long as you give appropriate credit to the original author(s) and the source, provide a link to the Creative Commons licence, and indicate if changes were made. The images or other third party material in this article are included in the article's Creative Commons licence, unless indicated otherwise in a credit line to the material. If material is not included in the article's Creative Commons licence and your intended use is not permitted by statutory regulation or exceeds the permitted use, you will need to obtain permission directly from the copyright holder. To view a copy of this licence, visit <http://creativecommons.org/licenses/by/4.0/>.

© The Author(s) 2024